ACS OMEGA

Open Access

http://pubs.acs.org/journal/acsodf

Article

OpenDEP: An Open-Source Platform for Dielectrophoresis Spectra Acquisition and Analysis

Ioan Tivig, Mihaela Georgeta Moisescu, and Tudor Savopol*

Cite This: *ACS Omega* 2023, 8, 38715−38722

Read Online

ACCESS | Metrics & More | Article Recommendations | Supporting Information

ABSTRACT: Dielectrophoretic (DEP) cell separation, which utilizes electric fields to selectively manipulate and separate cells based on their electrical properties, has emerged as a cutting-edge label-free technique. DEP separation techniques rely on differences in the electrical and morphological properties of cells, which can be obtained by a thorough analysis of DEP spectra. This article presents a novel platform, named OpenDEP, for acquiring and processing DEP spectra of suspended cells. The platform consists of lab-on-a-chip and open-source software that enables the determination of DEP spectra and electric parameters. The performance of OpenDEP was validated by comparing the results obtained using this platform with the results obtained using a commercially available device, 3DEP from DEPtech. The lab-on-a-chip design features two indium tin oxide-coated slides with a specific geometry, forming a chamber where cells are exposed to an inhomogeneous alternating electric field with different frequencies, and microscopic images of cell distributions are acquired. A custom-built software written in the Python programing language was developed to convert the acquired images into DEP spectra, allowing for the estimation of membrane and cytoplasm conductivities and permittivities. The platform was validated using two cell lines, DC3F and NIH 3T3. The OpenDEP platform offers several advantages, including easy manufacturing, statistically robust computations due to large cell population analysis, and a closed environment for sterile work. Furthermore, continuous observation using any microscope allows for integration with other techniques.

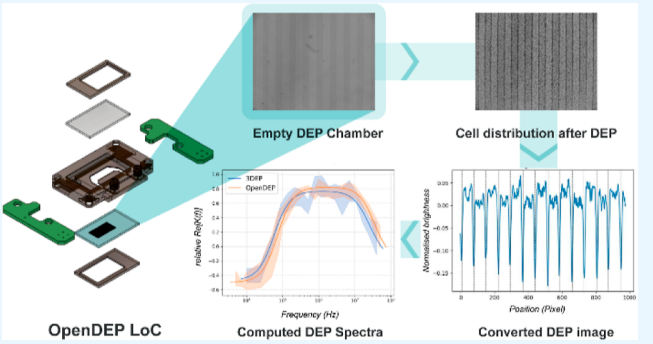

Label-free living cell separation represents a significant advancement in cellular analysis, offering researchers a powerful and versatile tool for studying cell populations in their native state. By eliminating the need for exogenous labeling, these methods preserve cellular integrity, enhance throughput, and enable real-time monitoring of dynamic cellular processes.[1,2]

Among these techniques, dielectrophoretic (DEP) cell separation is a cutting-edge technique that utilizes electric fields to selectively manipulate and separate cells based on their electrical properties.

Dielectrophoresis is the phenomenon by which a dielectric polarizable object placed in an inhomogeneous alternating electric field is experiencing a force, $\vec{F}_{DEP}$, according to the formula[3,4]

$$\vec{F}_{DEP} = 2\pi r^3 \varepsilon_0 \varepsilon_{med} Re[K(f)]\vec{\nabla}|E^2|$$

where r is the particle radius, ε_0 is the absolute electric permittivity of the vacuum, ε_{med} is the relative electric permittivity of the suspending medium, and E is the electric field intensity. $Re[K(f)]$ is the real part of the Clausius−Mossotti factor, which is a function of the frequency of the electric field, f. For a homogeneous spherical particle (carrying no charge and exhibiting no conductive losses), the Clausius−Mossotti factor is given by[4]

$$K(f) = \frac{\varepsilon_p^* - \varepsilon_{med}^*}{\varepsilon_p^* + 2\varepsilon_{med}^*}$$

where ε_p^* and ε_{med}^* are the complex permittivities of the particle and suspending medium, respectively; they both depend on the electric field frequency according to

$$\varepsilon_i^* = \varepsilon_i - \frac{\sqrt{-1}\,\sigma_i}{2\pi f}$$

where σ_i is the corresponding electric conductivity (i stands for either p or med).

For a more complex structure, better mimicking a living cell, like a homogeneous sphere surrounded by a shell (membrane), named "the single-shell model", the complex permittivity of the particle must be replaced by[4]

Received: August 16, 2023
Accepted: September 25, 2023
Published: October 6, 2023

https://doi.org/10.1021/acsomega.3c06052
ACS Omega 2023, 8, 38715−38722

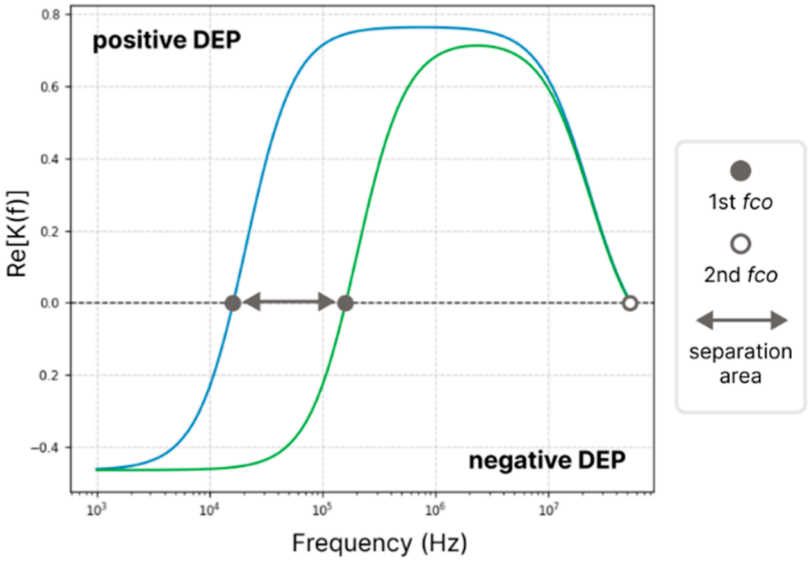

Figure 1. Example of DEP spectra of two types of cells that differ by their membrane permittivity, computed using the OpenDEP software (later to be presented). At low and high frequencies, the particles suffer negative DEP, while at intermediate frequencies, they suffer positive DEP. The blue trace corresponds to a relative membrane permittivity of 30 and the green one to 3. The gray arrow highlights the frequency range for which the two types of cells will experience opposite DEP forces.

$$\varepsilon_p^* = \frac{\left(\frac{r}{r-d}\right)^3 + 2\left(\frac{\varepsilon_i^* - \varepsilon_{mem}^*}{\varepsilon_i^* + 2\varepsilon_{mem}^*}\right)}{\left(\frac{r}{r-d}\right)^3 - \left(\frac{\varepsilon_i^* - \varepsilon_{mem}^*}{\varepsilon_i^* + 2\varepsilon_{mem}^*}\right)}$$

where r stands for the exterior radius of the particle, d for the thickness of the shell, and ε_i^* and ε_{mem}^* for the complex permittivities of the interior (cytoplasm) and the shell (membrane), respectively.

The frequency dependence of $Re[K(f)]$ represents the DEP spectrum of the particle. The general shape of this spectrum depends on the geometrical and electrical parameters of the suspended particles, as well as on the electrical parameters of the suspending medium.[5]

Figure 1 shows two DEP spectra computed based on the single-shell model.

One can see that there are frequency domains for which $Re[K(f)]$ has positive values and domains for which it has negative values. In the first situation, the DEP force has the same direction as the electric field gradient (situation called "positive DEP"), while in the latter, it has an opposite direction ("negative DEP"). At frequencies at which $Re[K(f)]$ is zero, called "crossover frequencies" (f_{co}), the particles do not experience any force.

It is worth noting that the first crossover frequency strongly depends on the electrical parameters of the shell (the blue trace in Figure 1, which corresponds to a membrane relative permittivity of 30, intersects the frequency axis at significantly lower values of the frequency than the green one, which is for a relative permittivity of 3). This observation is the basis of the cell separation methods by DEP because, exposed to an AC field, cells from a mixture will migrate in opposite directions, depending on whether their crossover frequencies are higher or lower than the applied frequency.

By exploiting the inherent differences in the electric properties of cells, DEP offers a label-free and noninvasive method for cell sorting and enrichment. This technique has found applications in various areas of research, including biomedicine,[6−8] tissue engineering,[9−12] and diagnostics,[10,13−15] and holds great promise for advancing our understanding of cellular behavior and disease processes.

Here, we propose a platform for DEP spectra acquisition and processing, named OpenDEP, which leads to a robust determination of the electric parameters of the cells. The platform is made of two components. A lab-on-a-chip (LoC) system integrating DEP electrodes allows the acquisition of microscopic images of the cell distribution under electric field exposure. A software, based on the processing of these images, computes DEP spectra and calculates the electric parameters of the cells. The platform has been used for acquiring and processing DEP spectra of NIH 3T3 and DC3F cells, and results were compared with those obtained with a commercially available device, 3DEP from DEPtech.[16]

OPENDEP LOC

Design and Simulation. The design (made in Autodesk Fusion 360 software) is composed of two main parts: the DEP characterization lab-on-a-chip (further named OpenDEP LoC) and its support (Figure 2).

The main body of the OpenDEP LoC (Figure 2b,c) acts like a separator between two indium tin oxide-coated slides (further named ITO electrodes), forming, together, a chamber where particles/cells are exposed to the electric field. The bottom ITO electrode (Figure 2b, band patterned ITO electrode) has areas where the ITO coating was removed in a line band pattern, thus obtaining alternative conductive and insulating parallel bands, each having a width of 0.25 mm. The top ITO electrode (Figure 2b, continuous ITO electrode) is continuous. The area on the chip where the distribution of the cells is monitored is ∼4 × 4 mm, if using a microscope objective of 4×. Simulations of the electric field intensities, made in COMSOL Multiphysics software (Figure 2d,e), reveal two advantages of this system: (i) apart from the DEP force exerted on the cells in the XY plane (that pushes cells horizontally toward the electrode edges), there is a component of the DEP force oriented downward the Z axis which forces them to gather in the focal plane of the microscope; (ii) there is a large area where cells are exposed to

https://doi.org/10.1021/acsomega.3c06052
ACS Omega 2023, 8, 38715−38722

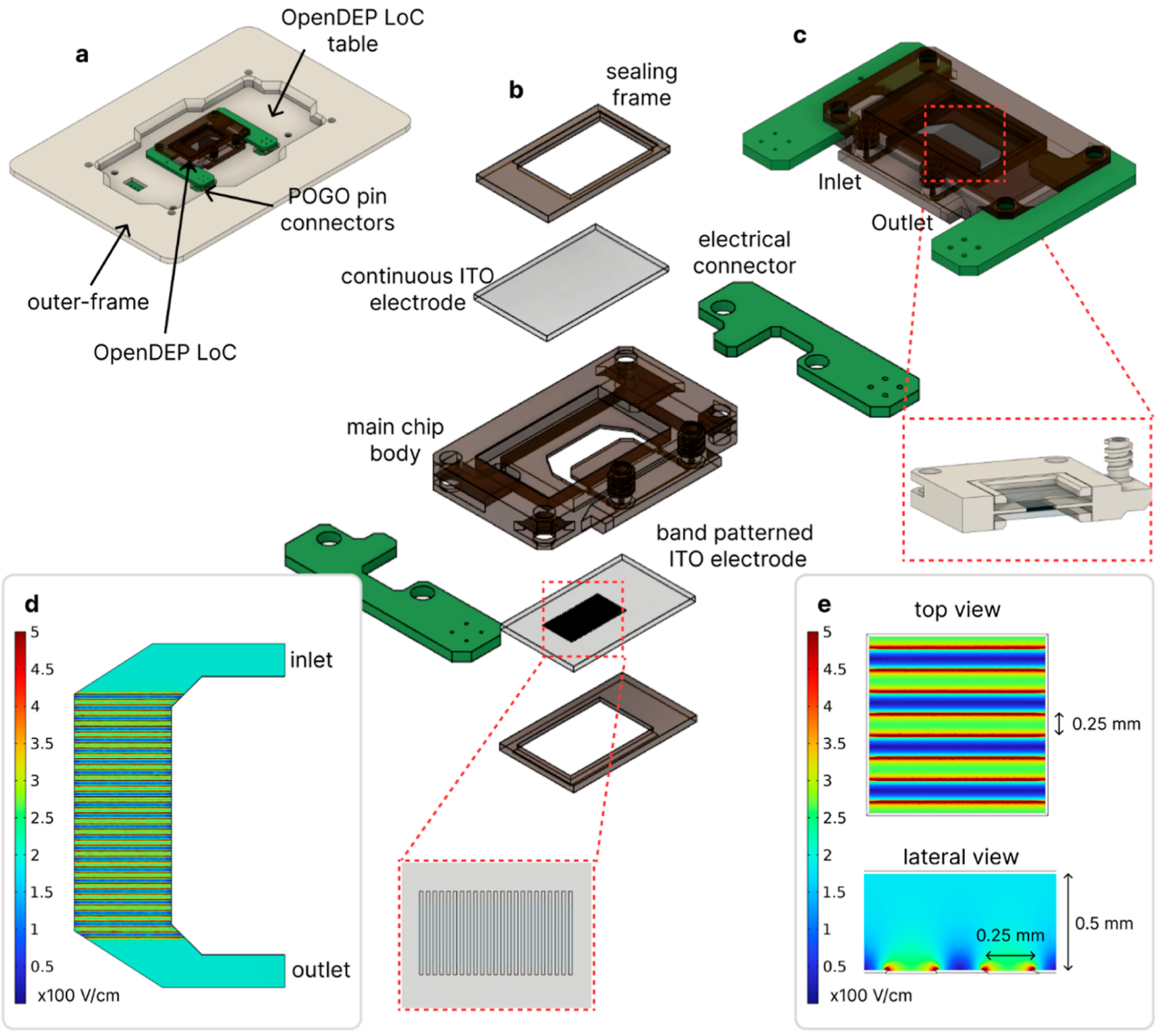

Figure 2. Schematics of the OpedDEP LoC [(a) the chip mounted on the table; (b) exploded draw of the chip with a zoom showing the band patterned bottom ITO electrode; and (c) assembled chip with a zoom showing a lateral section of the chip] and simulations of the electric field intensities generated by the two ITO electrodes [(d) the entire area where cells are exposed to the electric field and (e) detailed view of the electric field distribution from top and lateral].

the electric field and can be observed, allowing data acquisition on large populations and providing thus a robust evaluation of their distribution.

To ensure that the OpenDEP LoC is watertight, each electrode is sealed with a sealing frame. The fluidic inlet and outlet of the LoC are thread based.

For the electrical connection to the support, the LoC has two electrical connectors that push on the spring pin connectors of the OpenDEP LoC table (each in 4 points), thus ensuring good electrical contact. The OpenDEP LoC table (Figure 2a) has two roles: to easily connect the function generator to the OpenDEP LoC and to keep the LoC fixed on the microscope stage (during image acquisition). The support has an outer frame that is easily modifiable to fit most of the commercial microscopes.

Manufacturing. The main body of the OpenDEP LoC and the sealing frames were manufactured through LCD resin printing (Anycubic Photon Mono 4K, Hong Kong) from a negative photoresist (Anycubic UV tough resin). The frames were printed directly on the print bed, and the main body was supported by pillars at a 45° angle relative to the build plate. The slicing of the 3D model (exported as *.stl) was done with Chitubox slicing software (specifically designed for resin printing). After printing, the parts were washed for 10 min with absolute ethanol 99%, let dry for 10 min, and exposed to UV light (405 nm) for 20 min (the part was rotated after 10 min).

The electrodes were manufactured from indium tin oxide slides (ITO, 636916, Sigma-Aldrich, USA) cut into 15 mm × 25 mm pieces with a standard diamond glass cutter. To obtain the line band pattern on the bottom electrode, the ITO glass was coated with black paint (ONE black, Maston, Finland) and laser engraved on the areas where the ITO coating needed to be removed and incubated for 5 min at 45 °C in etching solution (2% $FeCl_3$ in 1:1 37% HCl/dH_2O). After incubation, the slides were washed with absolute ethanol to remove the paint coating. The laser engraving was done with a commercial consumer-grade 3 in 1 3D Printer (Snapmaker 2.0, China), and model

https://doi.org/10.1021/acsomega.3c06052
ACS Omega 2023, 8, 38715−38722

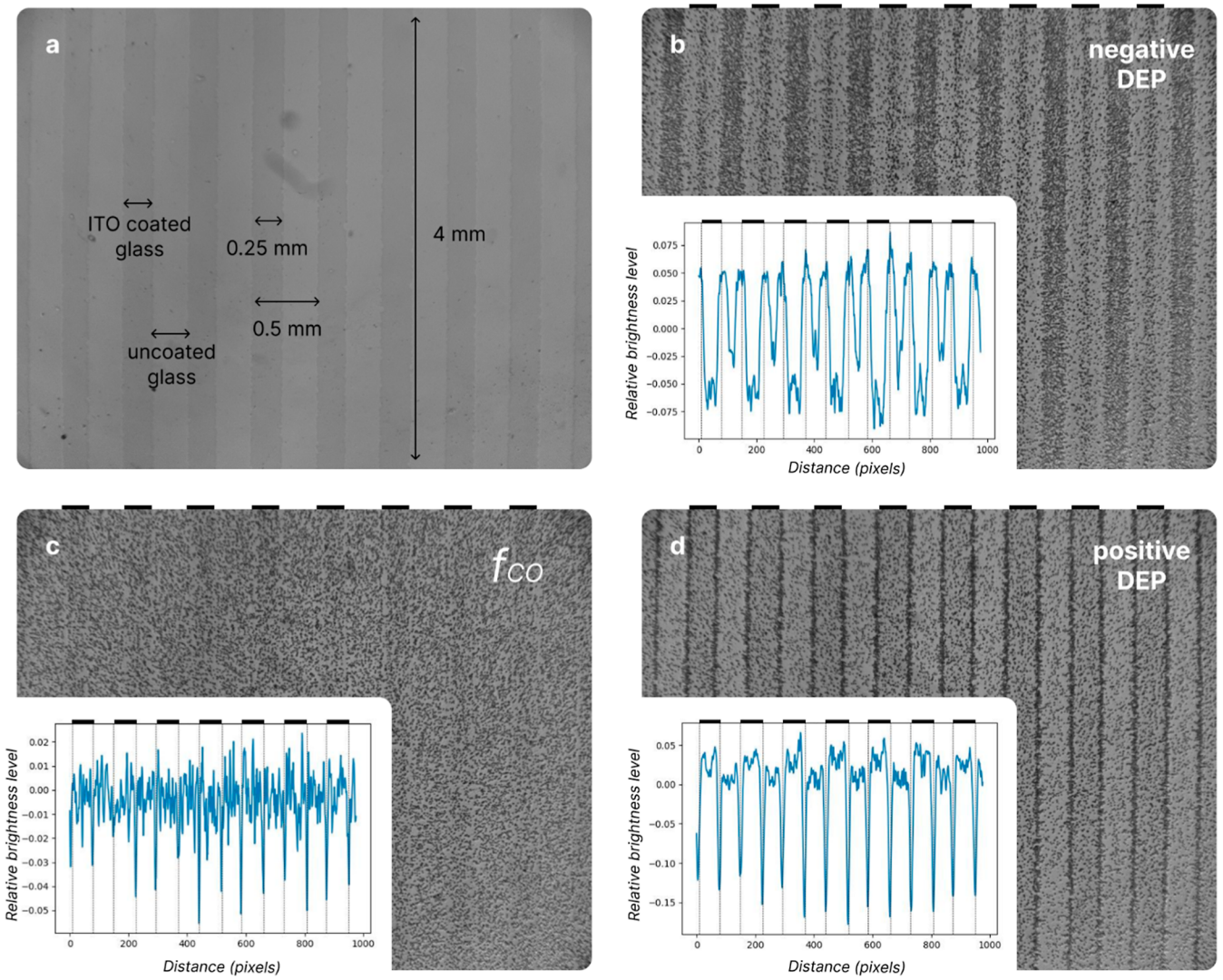

Figure 3. Images of the working area of the OpenDEP LoC. (a) Chip before adding the cell suspension, with the geometric characteristics of the electrodes; (b−d): images of the chip with cell suspension after applying the AC field of frequencies corresponding to negative DEP (with cells accumulating between the electrodes), f_{co} (with cells uniformly distributed), and positive DEP (with cells accumulating on the edges of electrodes), respectively (the position of the electrodes is represented as short black lines above each image). The insets show the corresponding relative brightness distribution averaged on rows of pixels (one pixel wide and along the whole height of the image) parallel to the electrodes as a function of the distance (in pixels) from the image left side.

processing was done prior to the engraving in Snapmaker Luban software.

The electrical connectors and the printed circuit board (PCB), which makes the connection between the function generator and the OpenDEP LoC, were carved with the drill carving module of the Snapmaker 2.0 machine. Two drill bits were used in the process: 0.5 and 0.8 mm flat drill bits made for carving PCBs. The PCB used was a standard copper-clad laminated board. The processing of the 3D model into the CNC machine code was done in Autodesk Fusion 360. The spring pins and the 3 pin connectors were soldered.

The OpenDEP LoC table and the outer frame were manufactured with polylactic acid (Snapmaker, China) with the 3D printing module of the Snapmaker machine. The slicing of the model was performed in Ultimaker Cura software.

All parts were kept in an assembled state with stainless steel screws.

Details and final product are presented in the Supporting Information file (Figure S2).

OPENDEP SOFTWARE

For the conversion of the microscopic images to $Re[K(f)]$, open-source software written in Python programing language was developed. It can be downloaded and freely used from the git hub page: https://github.com/IoanTivig/OpenDEP.git. The software is under GNU General Public License version 3. The software can fit the data with both the single shell and the homogeneous particle models and gives, as output parameters, the membrane and cytoplasm conductivities and permittivities.

To convert the images obtained with the OpenDEP LoC, the conversion module of the software computes an average of all the brightness values (with the pixel depths transformed in floating numbers between 0 and 1) on a row of pixels parallel to the electrodes and then represents these average values against the position of the rows along a direction perpendicular to the electrodes (Figure 3b−d).

Before the experiments are started, an image of the chamber with buffer (without cells) is taken (Figure 3a). This image is used by the software to localize the exact position of electrodes

https://doi.org/10.1021/acsomega.3c06052
ACS Omega 2023, 8, 38715−38722

Table 1. Input Parameters Used by the OpenDEP Software, Other than the Experimental Points Acquired on the LoC

parameters	values	cell line	observations
buffer permittivity	78	both	recommended by the 3DEP manufacturer
buffer conductivity	0.02, 0.04, 0.08 S/m	both	chosen based on the preliminary test
cytoplasm permittivity	40	both	recommended by the 3DEP manufacturer
cell radius	6.29 μm	NIH 3T3	measured
	7.18 μm	DC3F	
cell membrane thickness	6 nm	both	recommended by the 3DEP manufacturer

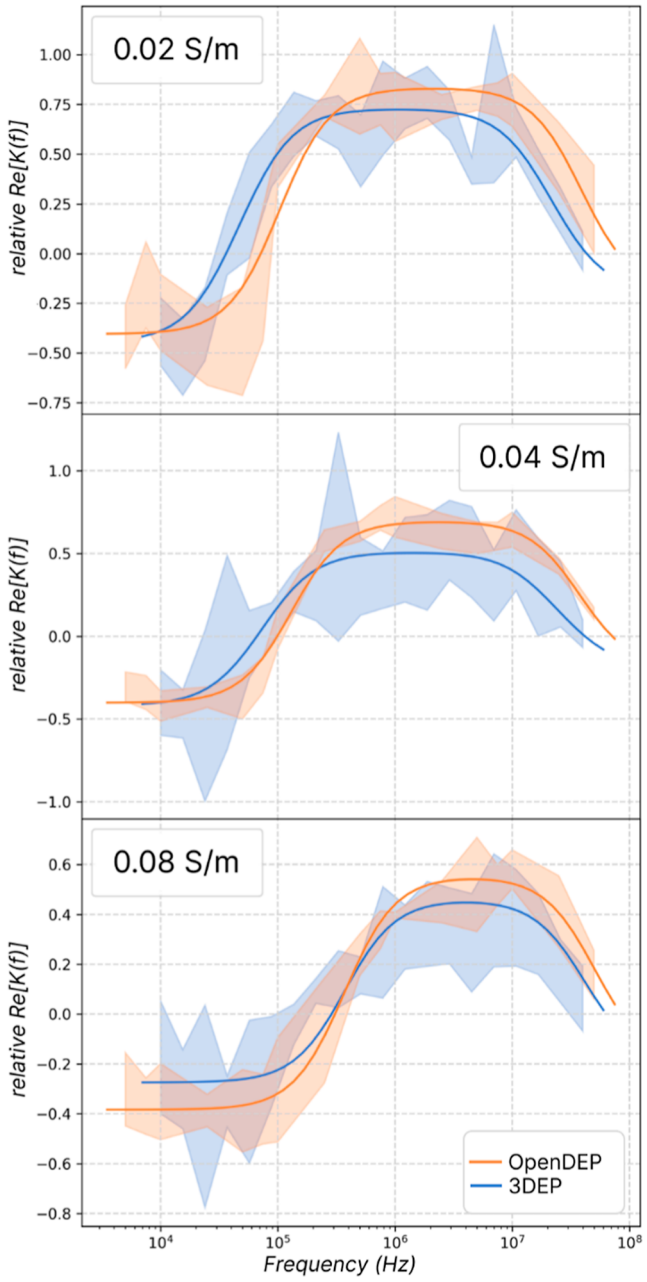

Figure 4. DEP spectra acquired on DC3F cells, suspended in three different conductivity buffers, using the 3DEP (blue trace) and Open DEP (orange trace) methods. The light-colored areas represent the corresponding standard deviations of the experimental points.

in the images, which will be later recorded on the chip containing cellular suspension. As long as the position of the chip is not modified, this image can be used for all subsequent image acquisition and processing. Then, the chip is filled with cellular suspension and a pair of images are acquired: one image before the exposure to the electric field and one after. Average brightness on rows of pixels (one pixel wide and along the whole height of the image) parallel to the electrodes is calculated on both images. The brightness values obtained before the cells exposure to the field are subtracted from those obtained after resulting in a relative brightness (insets in Figure 3b–d). Furthermore, the software calculates an average and a standard deviation of all relative brightness values positioned on or in proximity of the electrode's edges (the number of pixels on which the average is computed can be defined by the operator). The same procedure is done on pairs of images acquired for all the desired DEP frequencies.

Then, the software fits these average brightness values versus frequencies with the selected model (either single shell or homogeneous particle) based on the corresponding formula of $Re[K(f)]$ multiplied by a transformation factor. This transformation factor is allowed to vary to best fit the curve, and it is further used in the final transformation of brightness values into relative $Re[K(f)]$ values (by dividing the average brightness values to this factor).

After fitting, the software provides all of the parameters used in the process which were set to vary. The software allows the operator to set as fixed any parameter. The resulting parameters can be taken directly from the OpenDEP software graphical interface, or they can be exported to an.xlsx table.

CELLS

Two cell lines were used in experiments for validation of the system: DC3F (Chinese hamster lung fibroblast cell line) and NIH 3T3 (mouse embryonic fibroblast cell line). Both are frequently utilized in biological research and are renowned for their robust proliferation rates. Cells were grown in standard conditions (37 °C, 5% CO_2, humidified atmosphere).

Before the experiments, the cells were washed with 0.9% NaCl, detached with Trypsin-EDTA (Sigma T4174, USA), and suspended in DMEM (Sigma D5796, USA) supplemented with 10% fetal bovine serum (Sigma F7524, USA). The cell suspension was then centrifuged for 5 min at 300*g* at room temperature, the supernatant was discarded, and the cell pellet was gently washed three times with a 300 mM sucrose solution (pH 7.4, ~ 0.002 S/m, 300 mOsm/kg) while keeping it attached to the bottom of the tube. Finally, the pellet was resuspended in one of the following three DEP buffers with different conductivities: 0.02, 0.04, and 0.08 S/m. These DEP buffers were prepared by mixing two other buffers in different ratios: a saline sucrose solution (250 mM sucrose, 8 mM Na_2HPO_4, 2 mM KH_2PO_4, 1 mM $MgCl_2$, pH 7.4, ~ 0.128 S/m, 300 mOsm/kg) and the sucrose solution used in the washing step. Finally, the cell concentration was adjusted to ~5×10^6 cells/mL. The average size of the cells was measured (BioRad TC10 Automated Cell Counter, USA).

OBTAINING DEP SPECTRA

OpenDEP Platform. The cell suspension was loaded on the OpenDEP LoC, and images of the whole chip area were acquired before exposure and 60 s after exposure to an AC field set to a frequency ranging from 5 kHz to 50 MHz, 10 V peak to

https://doi.org/10.1021/acsomega.3c06052
ACS Omega 2023, 8, 38715−38722

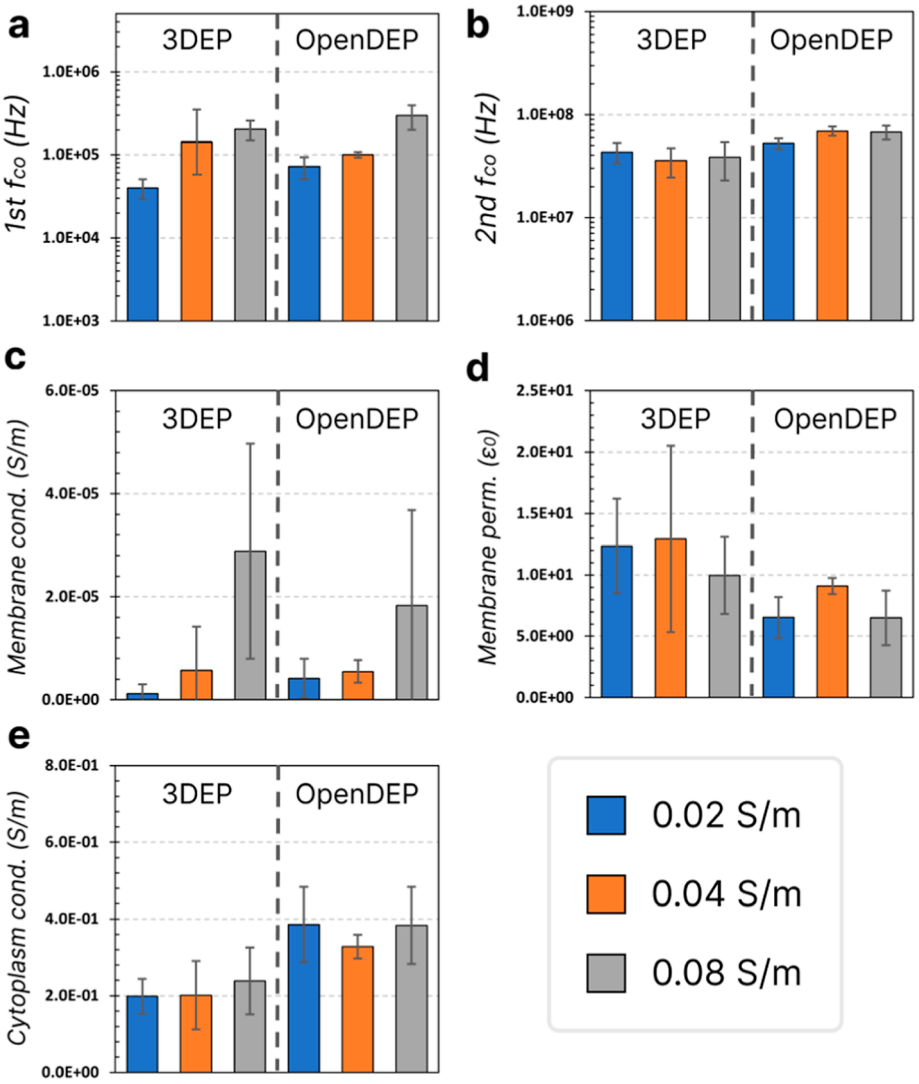

Figure 5. Electrical parameters of DC3F cells suspended in three different conductivity buffers, computed by OpenDEP, were based on data acquired using 3DEP and OpenDEP LoC. (a) 1st crossover frequency, (b) 2nd crossover frequency, (c) membrane conductivity, (d) membrane permittivity, and (e) cytoplasm conductivity.

peak. The AC field was generated by using a function generator (Agilent 33250A, USA), while image acquisition was performed by using an inverted microscope (Axiovert 200, Carl Zeiss, Germany). To ensure a homogeneous cell distribution between each acquisition of paired images, cells were mixed back and forth by using a syringe. For each frequency, the experiment was repeated at least four times. The images were subsequently converted into relative $Re[K(f)]$ using the OpenDEP software. The data were further processed (using the same software) to obtain the electric parameters of the cells.

3DEP Commercial Machine. For the validation of the OpenDEP system, DEP spectra were obtained using a 3DEP DEP analysis system (3DEP from DEPtech, UK) along with DEPwell 805 chips from the same manufacturer. These chips feature 20 wells equipped with a built-in electrode system, enabling the simultaneous application of different frequencies in each well. Sequential images were captured during application of the electric field for each well. Through analysis of the cell distribution evolution within each well, the system computed a dimensionless parameter, directly proportional to $Re[K(f)]$, named by producers "relative DEP force".[16]

Spectra were acquired at 20 frequencies spanning from 10 kHz to 40 MHz, with a recording duration of 60 s and a voltage of 10 V peak to peak. Each experiment was repeated at least five times. The data were subjected to further analysis using the OpenDEP software.

Data Processing. The input parameters required by the OpenDEP software are given in Table 1.

The data acquired with OpenDEP LoC were further processed according to the procedure described in the section OpenDEP Software.

For the 3DEP acquired data, the relative DEP force was converted to relative $Re[K(f)]$ using a dedicated conversion module of OpenDEP Software.

VALIDATION

Figure 4 shows the comparison of DEP spectra of DC3F cells suspended in three different conductivity buffers (0.02, 0.04, and 0.08 S/m) obtained by OpenDEP and 3DEP techniques (a similar example obtained on NIH 3T3 cell line is presented in the Supporting Information, Figure S4). For all external buffer

https://doi.org/10.1021/acsomega.3c06052
ACS Omega 2023, 8, 38715−38722

conductivities, the standard deviations of the experimental points overlap.

The good similarities of the spectra obtained by these two methods lead to good overlap of the computed parameters, as shown in Figure 5. The electric parameters computed by OpenDEP using the two spectra are in good agreement, although there are some small but systematic differences: membrane permittivity is slightly lower and cytosol conductivity is slightly higher when data were acquired with OpenDEP LoC compared to 3DEP.

Concerning the modifications of computed parameters induced by the suspending buffer conductivity, an almost perfect similarity between OpenDEP LoC and 3DEP can be observed: the first crossover frequency and the membrane conductivity increase with buffer conductivity (Figure 5a,c), while the other parameters remain unmodified (Figure 5b,d,e).

DISCUSSION AND CONCLUSIONS

In this paper, we presented an original platform for the acquisition and processing of dielectrophoresis spectra of suspended cells. The platform consists of a lab-on-a-chip and software that allows obtaining the dielectrophoresis spectra (and therefore the crossover frequencies) and, from the analysis of these spectra, obtaining the electric parameters of the cells. The platform was validated by comparing the results with those obtained, under identical conditions, using a commercial device (3DEP from DEPtech).

The most important advantages of the OpenDEP platform are the following:

- Its manufacture is very easy as it does not require special materials or techniques. It is modular and can be easily automated.
- The depth of the dielectrophoresis chamber is 500 μm, allowing the microscope to focus the image simultaneously on cells and electrodes.
- All computations are done on images acquired on a large surface of the chip, i.e., on a large population of cells, thus being statistically very robust. As a result, lower standard deviations were obtained by OpenDEP compared to 3DEP, despite the smaller number of samples used (see Figure 4, orange vs blue surfaces).
- Due to the geometry of the electrodes, the force generated in the case of both positive and negative DEP has a strong vertical component, directed downward, with the cells being thus directed to crowd in the lower plane of the chamber, i.e., in the focal plane, the image thus remaining permanently in focus, and the effects of gravitational deposition of cells thus being eliminated. It can be seen from Figure 2e (lateral view) that both the highest and lowest values of the electric field (red and blue, respectively) are localized in the proximity of the bottom of the chamber, in the same plane as the electrode's edges, the cells gathering thus at this level, and in a very thin layer, regardless of the fact whether they are subject to positive or negative DEP. The consequence is that the depth of the light scattering layer is very small, making the setup less prone to artifacts due to nonlinearity of the scattering if higher cellular concentrations are used.
- The LoC system allows working in a closed environment, so sterile work can be done (the chip itself is autoclavable if a proper photoresist is used).
- The LoC system allows continuous observation in any microscope, allowing the combination of DEP experiments with other applications (fluorescence microscopy, combined with optical tweezers, etc.).
- The software is open source.

The main disadvantage of OpenDEP LoC is that it requires successive image acquisition for each frequency to obtain a complete DEP spectrum. The acquisition of a whole spectrum typically takes 30 min compared to less than 1 min in the case of 3DEP for the same number of frequencies.

The OpenDEP LoC platform represents a valuable contribution to the presently existing devices used for the acquisition of DEP spectra using either single-cell[17−19] or populational techniques.[8,16,20,21] It represents a user-friendly platform to determine the electric parameters of cells.

ASSOCIATED CONTENT

Supporting Information

The Supporting Information is available free of charge at https://pubs.acs.org/doi/10.1021/acsomega.3c06052.

Images of the OpenDEP LoC divided into pieces, assembled, and mounted on the microscope; information regarding manufacturing; information regarding how to run the OpenDEP software and sort the data into folders for image conversion to relative $Re[K(f)]$ and electrical parameters computation; and data obtained on the NIH 3T3 cell line: spectra and electrical parameters obtained after fitting on three different conductivities (as in the case of the DC3F cell line) (PDF)

AUTHOR INFORMATION

Corresponding Author

Tudor Savopol − *Biophysics and Cellular Biotechnology Department, Excellence Center for Research in Biophysics and Cellular Biotechnology, Faculty of Medicine, Carol Davila University of Medicine and Pharmacy, Bucharest 050474, Romania;* orcid.org/0000-0001-7231-3581; Email: tudor.savopol@umfcd.ro

Authors

Ioan Tivig − *Biophysics and Cellular Biotechnology Department, Excellence Center for Research in Biophysics and Cellular Biotechnology, Faculty of Medicine, Carol Davila University of Medicine and Pharmacy, Bucharest 050474, Romania*

Mihaela Georgeta Moisescu − *Biophysics and Cellular Biotechnology Department, Excellence Center for Research in Biophysics and Cellular Biotechnology, Faculty of Medicine, Carol Davila University of Medicine and Pharmacy, Bucharest 050474, Romania;* orcid.org/0000-0003-0017-6180

Complete contact information is available at: https://pubs.acs.org/10.1021/acsomega.3c06052

Author Contributions

The manuscript was written through contributions of all authors. All authors have given approval to the final version of the manuscript. I.T. and M.G.M. equally contributed.

Notes

The authors declare no competing financial interest.

https://doi.org/10.1021/acsomega.3c06052
ACS Omega 2023, 8, 38715−38722

■ ACKNOWLEDGMENTS

The authors thank Dr. Lluis M. Mir, Directeur de Recherche CNRS at METSY, UMR 9018, Université Paris-Saclay, CNRS and Gustave Roussy, for offering the possibility to use the 3DEP DEPtech dielectrophoresis measurement system. The authors acknowledge financial support for the research activities from Unitatea Executivă pentru Finanţarea Învăţământului Superior, a Cercetării, Dezvoltării şi Inovării through the grant PN-III-P2-2.1-PED-2021-0451 (contract no. 596PED/2022), and from the European Social Fund "Net4SCIENCE: Applied doctoral and post-doctoral research network in the fields of smart specialization Health and Bioeconomy," project code POCU/993/6/13/154722. Publication of this paper was supported by the University of Medicine and Pharmacy Carol Davila through the institutional program Publish not Perish.

■ ABBREVIATIONS

DEP, dielectrophoresis; LoC, lab-on-a-chip; ITO, indium tin oxide; $Re[K(f)]$, real part of the Clausius-Mossotti factor

■ REFERENCES

(1) Sarno, B.; Heineck, D.; Heller, M. J.; Ibsen, S. D. Dielectrophoresis: Developments and Applications from 2010 to 2020. *Electrophoresis* **2021**, *42* (5), 539−564.
(2) Henslee, E. A. Review: Dielectrophoresis in Cell Characterization. *Electrophoresis* **2020**, *41* (21−22), 1915−1930.
(3) Pohl, H. A.; Pollock, K.; Crane, J. S. Dielectrophoretic Force: A Comparison of Theory and Experiment. *J. Biol. Phys.* **1978**, *6* (3−4), 133−160.
(4) Pethig, R. Review Article—Dielectrophoresis: Status of the Theory, Technology, and Applications. *Biomicrofluidics* **2010**, *4* (2), 022811.
(5) Gagnon, Z. R. Cellular Dielectrophoresis: Applications to the Characterization, Manipulation, Separation and Patterning of Cells. *Electrophoresis* **2011**, *32* (18), 2466−2487.
(6) Giduthuri, A. T.; Theodossiou, S. K.; Schiele, N. R.; Srivastava, S. K. Dielectrophoresis as a Tool for Electrophysiological Characterization of Stem Cells. *Biophys Rev.* **2020**, *1* (1), 011304.
(7) Giduthuri, A. T.; Theodossiou, S. K.; Schiele, N. R.; Srivastava, S. K. Dielectrophoretic Characterization of Tenogenically Differentiating Mesenchymal Stem Cells. *Biosensors (Basel)* **2021**, *11* (2), 50.
(8) Li, Y.; Wang, Y.; Wan, K.; Wu, M.; Guo, L.; Liu, X.; Wei, G. On the Design, Functions, and Biomedical Applications of High-Throughput Dielectrophoretic Micro-/Nanoplatforms: A Review. *Nanoscale* **2021**, *13* (8), 4330−4358.
(9) Huan, Z.; Ma, W.; Xu, M.; Zhong, Z.; Li, X.; Zhu, Z. Cell Patterning via Optimized Dielectrophoretic Force within Hexagonal Electrodes in Vitro for Skin Tissue Engineering. *Int. J. Adv. Manuf. Technol.* **2019**, *105* (12), 4899−4907.
(10) Çağlayan, Z.; Demircan Yalçın, Y.; Külah, H. A Prominent Cell Manipulation Technique in BioMEMS: Dielectrophoresis. *Micromachines (Basel)* **2020**, *11* (11), 990.
(11) Takeuchi, Y.; Miyata, S. Dielectrophoretic Micro-Organization of Chondrocytes to Regenerate Mechanically Anisotropic Cartilaginous Tissue. *Micromachines* **2021**, *12* (9), 1098.
(12) Wan Yahya, W. N.; Ibrahim, F.; Thiha, A.; Jamaluddin, N. F.; Madou, M. Fabrication of a 3D Carbon Electrode for Potential Dielectrophoresis-Based Hepatic Cell Patterning Application Using Carbon Micro-Electrical-Mechanical System (CMEMS). *J. Micromech. Microeng.* **2022**, *32* (5), 055005.
(13) Mohd Maidin, N. N.; Buyong, M. R.; Rahim, R. A.; Mohamed, M. A. Dielectrophoresis Applications in Biomedical Field and Future Perspectives in Biomedical Technology. *Electrophoresis* **2021**, *42* (20), 2033−2059.
(14) Bhat, M. P.; Thendral, V.; Uthappa, U. T.; Lee, K. H.; Kigga, M.; Altalhi, T.; Kurkuri, M. D.; Kant, K. Recent Advances in Microfluidic Platform for Physical and Immunological Detection and Capture of Circulating Tumor Cells. *Biosensors (Basel)* **2022**, *12* (4), 220.
(15) Russo, G. I.; Musso, N.; Romano, A.; Caruso, G.; Petralia, S.; Lanzanò, L.; Broggi, G.; Camarda, M. The Role of Dielectrophoresis for Cancer Diagnosis and Prognosis. *Cancers (Basel)* **2021**, *14* (1), 198.
(16) Hoettges, K. F.; Henslee, E. A.; Torcal Serrano, R. M.; Jabr, R. I.; Abdallat, R. G.; Beale, A. D.; Waheed, A.; Camelliti, P.; Fry, C. H.; van der Veen, D. R.; Labeed, F. H.; Hughes, M. P. Ten-Second Electrophysiology: Evaluation of the 3DEP Platform for High-Speed, High-Accuracy Cell Analysis. *Sci. Rep.* **2019**, *9* (1), 19153.
(17) Marszalek, P.; Zielinsky, J. J.; Fikus, M.; Tsong, T. Y. Determination of Electric Parameters of Cell Membranes by a Dielectrophoresis Method. *Biophys. J.* **1991**, *59* (5), 982−987.
(18) Kaler, K. V.; Jones, T. B. Dielectrophoretic Spectra of Single Cells Determined by Feedback-Controlled Levitation. *Biophys. J.* **1990**, *57* (2), 173−182.
(19) Jeon, H. J.; Lee, H.; Yoon, D. S.; Kim, B. M. Dielectrophoretic Force Measurement of Red Blood Cells Exposed to Oxidative Stress Using Optical Tweezers and a Microfluidic Chip. *Biomed Eng. Lett.* **2017**, *7* (4), 317−323.
(20) Hoettges, K. F.; Hübner, Y.; Broche, L. M.; Ogin, S. L.; Kass, G. E. N.; Hughes, M. P. Dielectrophoresis-Activated Multiwell Plate for Label-Free High-Throughput Drug Assessment. *Anal. Chem.* **2008**, *80* (6), 2063−2068.
(21) Fatoyinbo, H. O.; Hoettges, K. F.; Hughes, M. P. Rapid-on-Chip Determination of Dielectric Properties of Biological Cells Using Imaging Techniques in a Dielectrophoresis Dot Microsystem. *Electrophoresis* **2008**, *29* (1), 3−10.

https://doi.org/10.1021/acsomega.3c06052
ACS Omega 2023, 8, 38715−38722